

Effect of heat treatment on microstructures and mechanical properties of sand-cast Mg–10Gd–3Y–0.5Zr magnesium alloy

Liang CAO¹, Wen-cai LIU^{1,2}, Zhong-quan LI³, Guo-hua WU^{1,2}, Lü XIAO³, Shao-hua WANG⁴, Wen-jiang DING^{1,2}

1. National Engineering Research Center of Light Alloy Net Forming,
Shanghai Jiao Tong University, Shanghai 200240, China;

2. Key State Laboratory of Metal Matrix Composite, Shanghai Jiao Tong University, Shanghai 200240, China;

3. Shanghai Aviation Precision Machinery Research Institute, Shanghai 201600, China;

4. Science and Technology on Space Physics Laboratory, Beijing 100076, China

Received 8 April 2013; accepted 5 July 2013

Abstract: The microstructure, mechanical properties and fracture behavior of sand-cast Mg–10Gd–3Y–0.5Zr alloy (mass fraction, %) under T6 condition (air cooling after solid solution and then aging heat treatment) were investigated. The optimum T6 heat treatments for sand-cast Mg–10Gd–3Y–0.5Zr alloy are (525 °C, 12 h + 225 °C, 14 h) and (525 °C, 12 h + 250 °C, 12 h) according to age hardening curve and mechanical properties, respectively. The ultimate tensile strength, yield strength and elongation of the Mg–10Gd–3Y–0.5Zr alloy treated by the two optimum T6 processes are 339.9 MPa, 251.6 MPa, 1.5% and 359.6 MPa, 247.3 MPa, 2.7%, respectively. The tensile fracture mode of peak-aged Mg–10Gd–3Y–0.5Zr alloy is transgranular quasi-cleavage fracture.

Key words: Mg–10Gd–3Y–0.5Zr; magnesium alloy; heat treatment; fracture; microstructure; mechanical property

1 Introduction

Magnesium and its alloys are the lightest metal structure materials in the current applications, and have irreplaceable functions compared with aluminum and steel such as high specific strength, high thermal conductivity, high static electricity shielding, high machining quality and very low density. The magnesium alloys are widely used in aeronautics, automobile, computer, communication and appliance industry, being praised of the green engineering material in the 21st century. It has been demonstrated that rare earth metals (RE) are the most effective elements to improve the strength properties of magnesium especially [1]. The strength of the Mg–RE alloys is achieved essentially via precipitation hardening, which is higher than that of conventional Al and Mg alloys [2]. Among different kinds of Mg–RE alloys [3–7], Mg–Gd–Y system is one of the most promising candidates due to its rapid age-hardening response and very good thermal stability

of the main strengthening phase up to 250 °C. Many investigations related to the microstructure and mechanical properties of the Mg–Gd–Y system have been reported [8–10]. ANYANWU et al [11] reported that Mg–10Gd–3Y–0.5Zr alloy has excellent strength, elongation and creep resistance in the peak-aging condition, which is superior to WE54 and WE43. Therefore, it becomes a research focus in the area of rare earth magnesium alloys.

Traditionally, water cooling is an effective way to inhibit growth of grains and improve alloy strength. However, water cooling can lead to stress residue and stress concentration in alloys, which causes the lift of brittleness to some extent. Mg–RE alloys are attractive in aerospace and aircraft industries for their low densities, high tensile strength and high creep resistance. As Mg–RE tools and structural components are becoming more and more complicated, a problem is recently found that cracks even fractures are sometimes observed in sand-cast complicated structural components when water cooling is taken after heat treatment, which

Foundation item: Project (51275295) supported by the National Natural Science Foundation of China; Project (USCAST2012-15) supported by the Funded Projects of SAST-SJTU Joint Research Centre of Advanced Aerospace Technology, China; Project (20120073120011) supported by the Research Fund for the Doctoral Program of Higher Education of China

Corresponding author: Wen-cai LIU; Tel: +86-21-54742630; E-mail: liuwc@sjtu.edu.cn

DOI: 10.1016/S1003-6326(14)63102-2

indicates that traditional water cooling process is not suitable for sand-cast complicated structural components after heat treatment. Air cooling is verified to be an effective cooling method to solve the crack problem through practice.

However, few systematical research reports on heat treatment process of air cooling and subsequent microstructures, mechanical properties and fracture behavior are found. The present study is aimed to optimize heat treatment process, based on air cooling, of sand-cast Mg–10Gd–3Y–0.5Zr (named as GW103K) and investigate its corresponding microstructure, mechanical properties at room temperature and fracture behavior by various analysis methods.

2 Experimental

The material used in this study is an Mg–10Gd–3Y–0.5Zr (mass fraction, %) alloy, produced by sand mould casting. As the components of the study alloy are accordance with the alloys used in engines and bodies of missiles in aerospace projects, this study can guide appliance in reality. According to the results by WANG [12], HE et al [13,14] and DRITS et al [15] and Mg–Gd–Y ternary phase diagram, the temperature of solution heat treatment was determined to be 525 °C and the time was 12 h. After solid solution, the specimens were cooled to room temperature in the air. Subsequently, specimens were isothermally aged at 225 °C and 250 °C respectively for different time in oil-bath furnace. Aged specimens were taken Vickers hardness testing, which used 49 N of load on the specimens for 20 s, to check the aging response.

Specimens for mechanical testing were machined with the load axis parallel to cast direction (CD) of the cast bars. Tensile properties of the tested alloys were performed at the initial strain rate of $5 \times 10^{-4} \text{ s}^{-1}$ referred to GB/T2008—2002 using cylindrical specimen (see Fig. 1) with marked dimensions of 33 mm in gauge length and 5 mm in diameter on Zwick/Roell Z020 tensile machine at room temperature. Microstructure of the studied alloys was observed by an optical microscope (OM). Phase compositions were scanned by X-ray diffractometer. The fracture surface and profiles were analyzed by a scanning electron microscope (SEM).

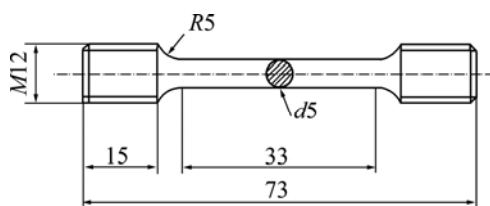


Fig. 1 Shape and size of cylindrical tensile specimen (unit: mm)

3 Results and discussion

3.1 Microstructures

The microstructures and phase compositions of the sand-cast and solution heat treated (T4: 525 °C, 12 h) GW103K alloys by OM and XRD analyses are shown in Figs. 2 and 3, respectively. As shown in Fig. 2(a), the microstructure of the sand-cast GW103K alloy consists of equiaxed α -Mg matrix and network eutectic compounds which distribute at grain boundaries. The secondary phase is observed and little pseudo eutectic or dendrite is found in the alloy. The grains' shapes of the

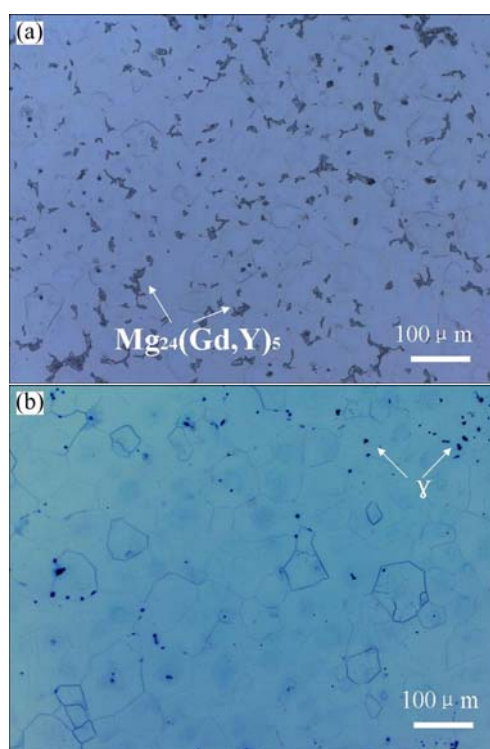


Fig. 2 OM images of sand-cast (a) and T4 treated (525 °C, 12 h) (b) GW103K alloy

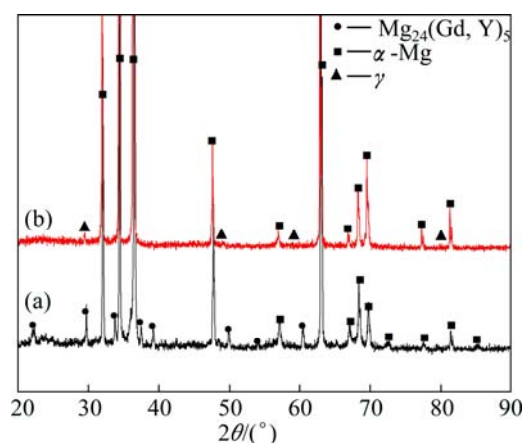


Fig. 3 XRD patterns of sand-cast (a) and T4 treated (b) GW103K alloy

sand-cast alloy is polygons and their boundaries are very clear. The microstructure after solution treatment of (525 °C, 12 h) is shown in Fig. 2(b). Almost all the eutectic compounds have been dissolved into the matrix. Gd and Y atoms dissolved into the magnesium matrix and formed supersaturated solid solution. Compared with WANG's result [12] of the T4 treated GW103K alloy which was carried out water cooling after solution heat treatment, the microstructure in this work which used air cooling after solution appears to be more homogeneous and there is less secondary phase retained. Moreover, some unevenly distributed small granular black dots are observed along grain boundaries and inside the grains. These dots are cluster remnant secondary phase and small cuboid-shaped phase (γ phase). Based on the results by WANG [12] and HE [14], small cuboid-shaped phase is a compound with high contents of rare earth elements and its size is 2–5 μm . It has face-centered cubic structure and the lattice constant is 5.6 Å. The corresponding XRD analysis results of the sand-cast and solution treated GW103K alloy are shown in Fig. 3. It can be seen that the sand-cast GW103K alloy contains two different phases: α -Mg phase and the eutectic phase consisting of $\text{Mg}_{24}(\text{Gd},\text{Y})_5$. Compared with the sand-cast alloy, the peak of eutectic phase $\text{Mg}_{24}(\text{Gd},\text{Y})_5$ almost disappears in the solution treated alloy. Meanwhile, the peak of γ phase appears. According to XRD results, the main composition of T4 treated GW103K alloy is α -Mg and γ phase. There is no diffraction peak of γ phase in

sand-cast alloy, which means that the amount of small cuboid-shaped phase is too little. Therefore, most of small cuboid-shaped phases are produced during solution heat treatment.

Figure 4 shows the microstructures of sand-cast T6 treated (solution: 525 °C, 12 h) GW103K alloy. As seen from Figs. 4(a)–(c), no significant change in morphology is observed in terms of grain size after aging heat treatment. Small granular black dots dispersively distributed both in grains and at grain boundaries after aging 225 °C while they mostly segregated at grain boundaries after aging at 250 °C. Besides, some Zr cores are also observed inner the grain of alloys aged at 250 °C. The corresponding XRD analysis towards the T6 treated GW103K alloy is presented in Fig. 5. It can be seen that β'' and β' phases are detected. With the increase of aging time from under-aging to peak-aging period, the peaks of β'' phase gradually disappear and the peaks of β' phase appear. The precipitation sequence of GW103K is: α -Mg supersaturated solid solution (S.S.S.S.) \rightarrow metastable β'' (D0_{19}) \rightarrow metastable β' (cbco) \rightarrow metastable β_1 (fcc) \rightarrow stable β (fcc). The metastable β' phase is regarded as the main strengthening phase in Mg–Gd alloys [14]. The diffraction peaks of small cuboid-shaped phase are detected at the range of 28°–30° and 47°–49°, which are also detected in the XRD patterns of solution treated GW103K alloy. This indicates that aging heat treatment cannot eliminate the γ phase produced in the solution heat treatment, which accords with the results of

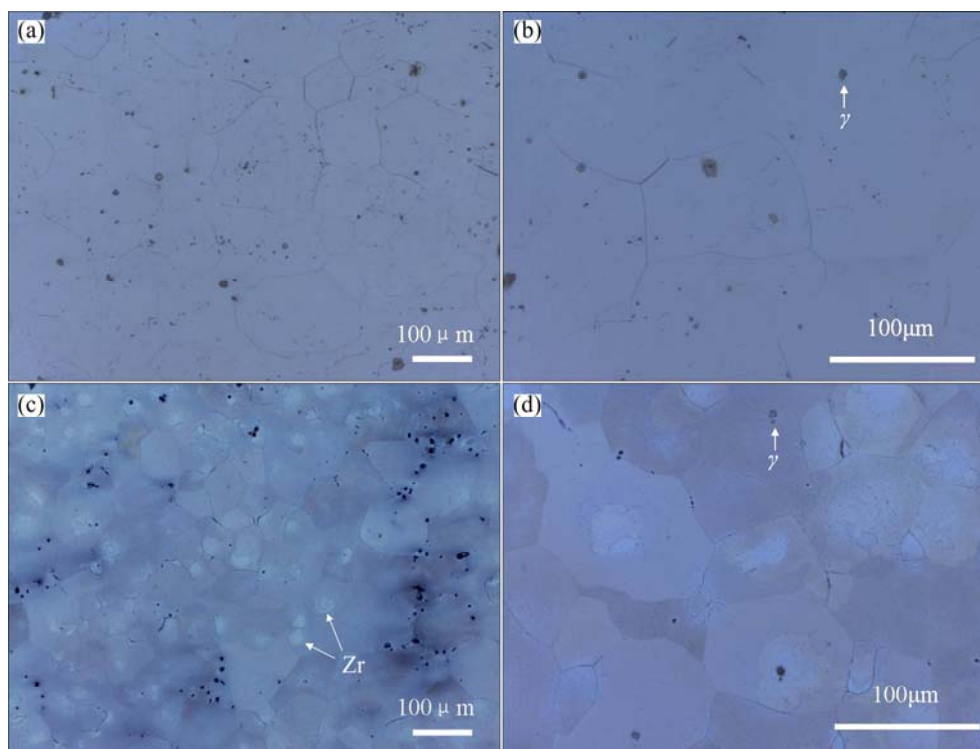


Fig. 4 Microstructures of T6 treated GW103K alloy under different aging conditions with various amplifications: (a, b) 225 °C, 14 h; (c, d) 250 °C, 12 h

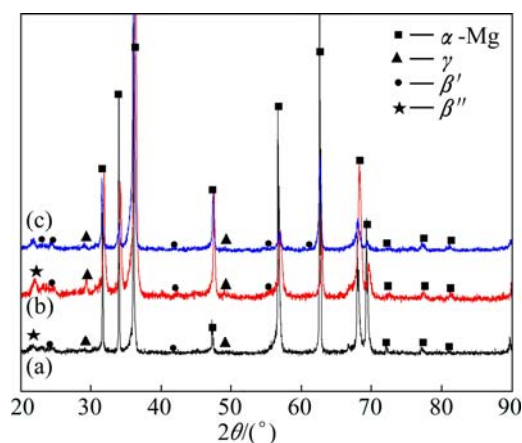


Fig. 5 XRD patterns of T6 treated GW103K alloy under different aging conditions: (a) 225 °C, 4 h; (b) 225 °C, 8 h; (c) 225 °C, 14 h

microstructure observation. Therefore, the microstructure of peak-aging GW103K alloy mainly consists of α -Mg, γ and β' .

3.2 Aging hardening

Figure 6 shows the aging hardness curves of the solution-treated (T4: 525 °C, 12 h) GW103K alloys. The hardness of solution treated alloy is HV82.7. In the process of aging, the hardness increases with the increase of aging time before reaching the peak hardness. Continuing ageing leads to the coarsening of β' phase [16] and the formation of stable β phase [17], which causes the hardness to decrease evidently. The hardness of alloy aged at 225 °C is superior to that aged at 250 °C. The alloy aged at 225 °C takes 14 h to reach the peak hardness of HV120.9, which is HV10 higher than the peak hardness of the alloy aged at 250 °C for 12 h. Therefore, the heat treatment condition of (525 °C, 2 h + 225 °C, 14 h) is selected as the optimum heat treatment of GW103K alloy according to Vickers

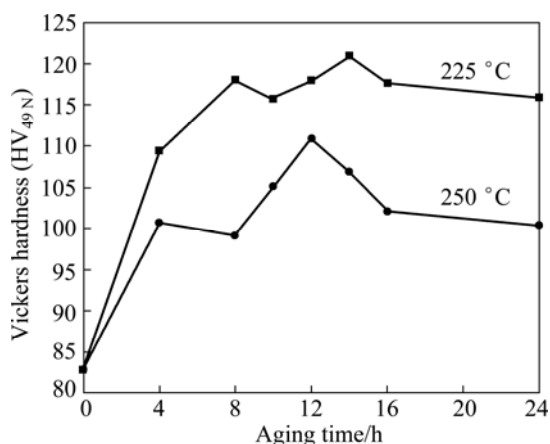


Fig. 6 Aging hardness curves of solution treated (525 °C, 12 h) GW103K alloy at aging temperature of 225 °C and 250 °C

hardness test results. Compared with the hardness of as-cast GW103K alloy (HV85.4), the peak hardnesses at two aging treatment temperatures increase by 41.6% and 29.9%, respectively, showing obvious aging hardening behavior.

3.3 Tensile properties

Figure 7 and Table 1 show tensile properties of GW103K alloy at room temperature under different aging conditions. Large improvement of the yield strength (YS) and the ultimate tensile strength (UTS) is observed with increasing the aging time before reaching the peak-aging state, which can be explained by precipitation behavior. After peak-aging point, YS and UTS gradually decrease due to the decrease in amount of strengthening phase β' caused by over aging. Because of high content of heavy rare earth elements, elongation (EL) of GW103K alloy is comparatively low. The maximum YS, UTS and EL of alloy are 251.6 MPa, 339.9 MPa and 1.5% aged at 225 °C for 14 h and 247.3 MPa, 359.6 MPa and 2.7% aged at 250 °C for 12 h. Overall, the YS of the test alloy aged at 225 °C is better than that aged at 250 °C, while UTS and EL are inferior. Compared with the YS, UTS and EL of as-cast and solution-treated GW103K alloy of which are 182 MPa, 220 MPa, 1.1% and 173 MPa, 230 MPa, 4.8%, respectively, the strength of the T6-treated GW103K alloy shows large improvement and the toughness of the alloy increases little compared with as-cast alloy but decreases compared with solution-treated alloy. Precipitation strengthening of the alloying elements Gd and Y is the main strengthening mechanism in GW103K alloy [1,18]. According to the former results of phase analysis and microstructure, the precipitates of the alloy aged at 250 °C remain tinier and dispersively distribute at grain boundaries, which can enhance the strengthening effect of grain boundaries. The strong grain boundaries become obstacles for dislocations to move so that the strength of alloy is intensified, which contributes to the higher intensity of alloy aged at 250 °C. Therefore, the process of (525 °C, 12 h + 250 °C, 12 h) is regarded as the optimized heat treatment condition according to tensile properties, and the process of (525 °C, 12 h + 225 °C, 14 h) can be adopted in applications when YS of the alloy is primarily required. Besides, in this work, the T6-treated GW103K alloy shows higher EL in tensile test at room temperature compared with that water cooled both after solution and aging treatment according to Refs. [12,14]. This indicates that the slower cooling process of air cooling can reduce the stress concentration and increase toughness of the GW103K alloy, which can explain that air cooling is an effective way to prevent crack from forming in complicated structural

components. Comparatively, the strength of peak-aged GW103K alloy by water cooling method after heat treatment is higher [14].

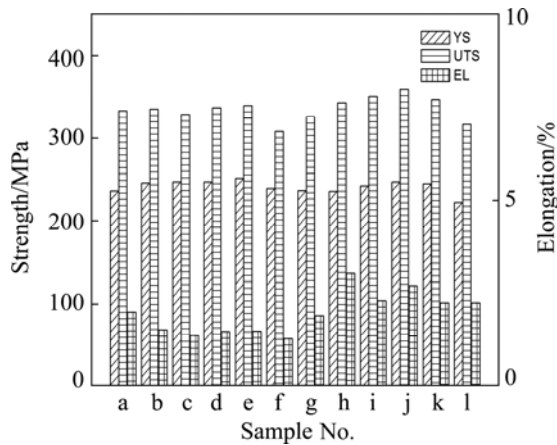


Fig. 7 Tensile properties of solution-treated GW103K alloys after different aging treatment conditions at room temperature

Table 1 Tensile properties of solid-solution and aging treated GW103K alloy

No.	Aging condition	YS/MPa		UTS/MPa		EL/%	
		Mean	STD	Mean	STD	Mean	STD
a	225 °C, 4 h	236.4	3.9	333.4	1.5	1.9	0
b	225 °C, 8 h	246.2	3.2	335.5	16.0	1.5	0.2
c	225 °C, 10 h	247.4	3.2	328.8	3.6	1.4	0.2
d	225 °C, 12 h	247.6	1.9	337.0	6.5	1.5	0.1
e	225 °C, 14 h	251.6	7.1	339.9	5.4	1.5	0.1
f	225 °C, 64 h	239.5	2.1	308.4	17.3	1.3	0.2
g	250 °C, 4 h	236.9	5.2	326.1	3.3	1.9	0.6
h	250 °C, 8 h	236.3	8.9	343.2	7.2	3.0	1.0
i	250 °C, 10 h	242.8	3.5	350.9	6.6	2.3	0.5
j	250 °C, 12 h	247.3	2.9	359.6	10.1	2.7	0.7
k	250 °C, 14 h	245.1	3.7	346.9	6.0	2.2	0.7
l	250 °C, 64 h	222.5	3.5	317.2	9.3	2.2	0.1

STD refers to the standard deviation from the mean value.

Some secondary phases of solution-treated GW103K alloy are observed. By contrast, no such phenomenon of existing secondary phase in solution-treated GW103K alloy water cooled after heat treatment is described towards T4 treated Mg–Gd–Y alloys using water cooling after heat treatment [12,19]. Therefore, it is believed that the secondary phase precipitates in the process of air cooling. Due to its slow cooling rate, air cooling process acts as function of a short period of aging. Referred to Ref. [17], β' forms during a very short time of aging. As precipitation strengthening is reported to be the main strengthening mechanism in Mg–Gd–Y alloys, the secondary phases like β' and β'' precipitate

and become obstacles for dislocations to move, which can effectively enhance the strength of the alloy. Tensile tests of solution-treated GW103K alloy by different cooling ways were carried out (see Fig. 8). It is observed that the mechanical properties of the alloy air cooled after solution treatment is notably superior to the alloy water cooled after solution treatment.

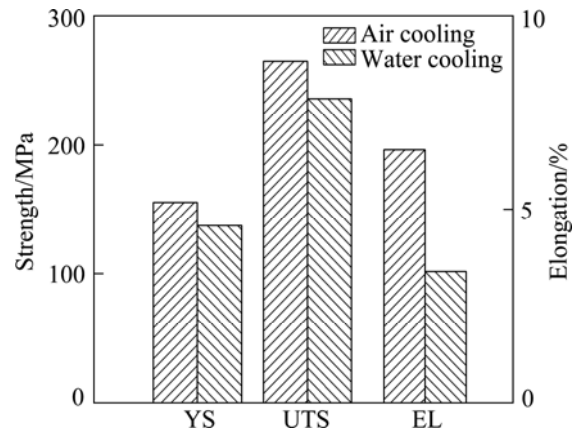


Fig. 8 Tensile properties of solution-treated GW103K alloys after different cooling methods at room temperature

3.4 Fractography

Figure 9 shows the fracture surfaces of the tensile specimens in different conditions. The whole fracture surface inclines to the loading axis and is close to the plane with the maximum shear force. It is observed that there are some cleavage planes and evident tearing ridges on the fracture surfaces of specimens peak-aged at 225 °C for 14 h. A few dimples and microporosities are observed as well. Comparatively, less cleavage planes are shown on the fracture surfaces of specimens peak-aged at 250 °C for 12 h. The fracture surface is mainly composed of many dispersed and tiny dimples. Therefore, the fracture mode of peak-aging alloys are transgranular quasi-cleavage fractures and mixture of brittle fracture and ductile fracture, and the toughness of GW103K alloy aged at 250 °C is superior to that aged at 225 °C, which is in accordance with the tensile test results. Some small cuboid particles, which are γ particles, are observed in the dimples. Some broken γ particles can also be observed, which indicates that the γ phase particles do not have significant strengthening effects, but the elastic strain energy of these particles releases and dimples form during tensile process. Figure 10 shows the comparison of the fracture surface of specimens under-aged at 225 °C for 4 h and peak-aged at 225 °C for 14 h. It is obvious that the fracture surface of under-aged alloy is composed of massive cleavage planes and grain boundaries, which indicates that the fracture mode is typical transgranular cleavage fracture while less cleavage planes, grain boundaries

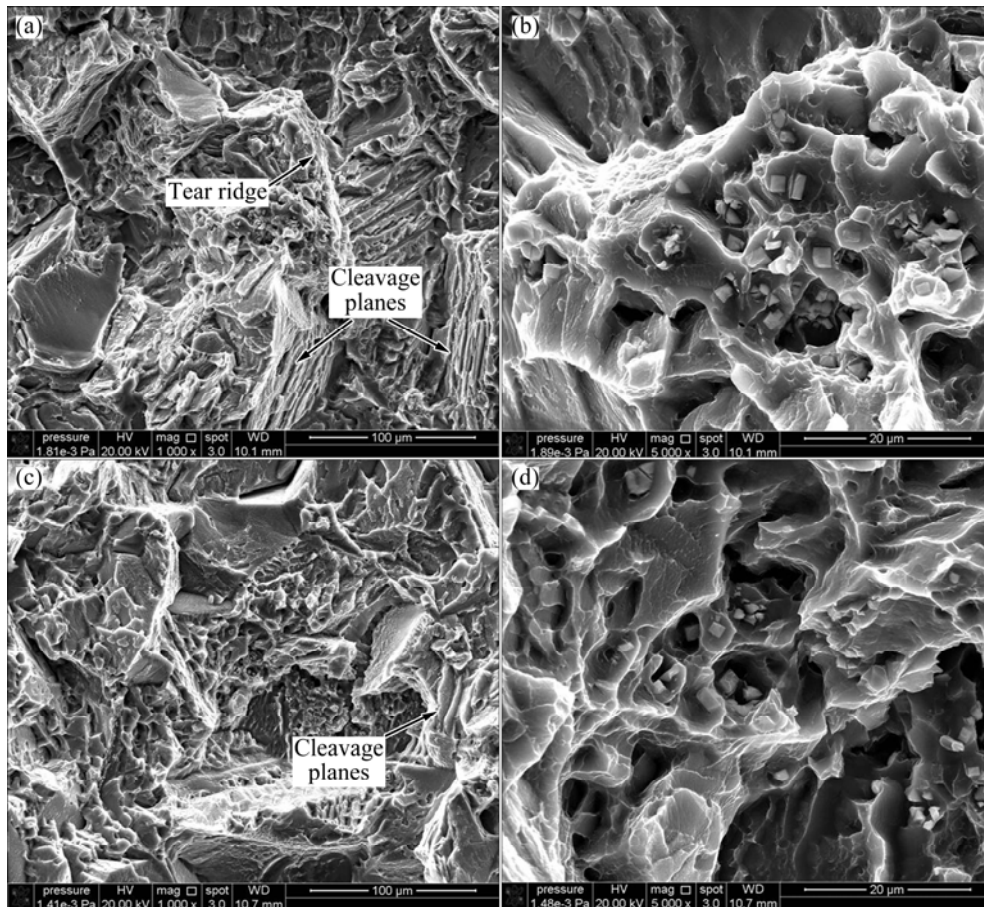


Fig. 9 Typical SEM images showing fracture surfaces of specimens under different conditions: (a) Peak-aging at 225 °C; (b) Magnified view of central region in (a); (c) Peak-aging at 250 °C; (d) Magnified view of central region in (c)

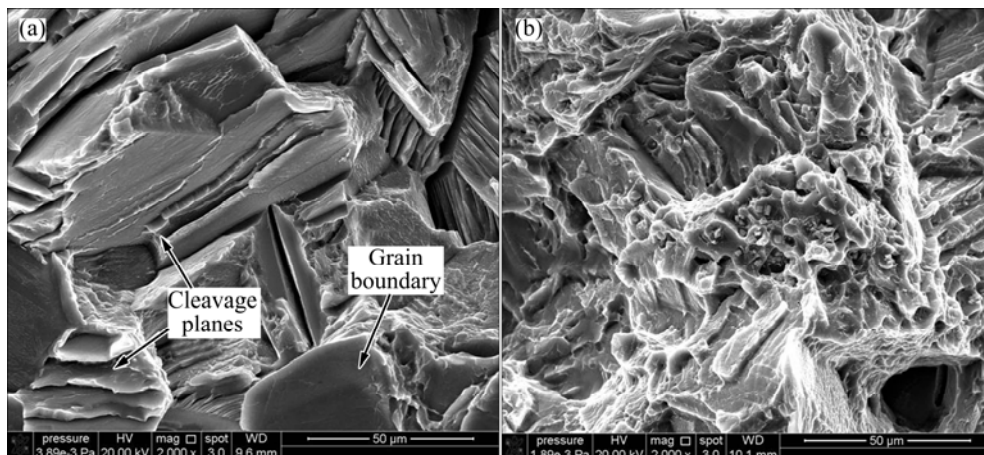


Fig. 10 Typical SEM images showing fracture surfaces under different conditions: (a) Under-aging at 225 °C; (b) Peak-aging at 225 °C

comparatively and some dimples in the fracture of peak-aged alloy show that the fracture mode is transgranular quasi-cleavage fracture. This indicates that the toughness of sand-cast GW103K alloy improves with the progress of aging heat treatment, which is consistent with results in Refs. [12,14,20].

Figure 11 shows the microstructures of fracture surface of GW103K alloy under different aging

conditions. The specimens show the secondary crack morphologies. Apparent transgranular secondary cracks from both microstructures of alloys aged at 225 °C and 250 °C are observed, which indicates that fracture mode of T6 treated GW103K alloy is mainly transgranular fracture. Inside some grains, a large number of fine twins are observed. Twinning is an especially important deformation mechanism for HCP magnesium alloys, in

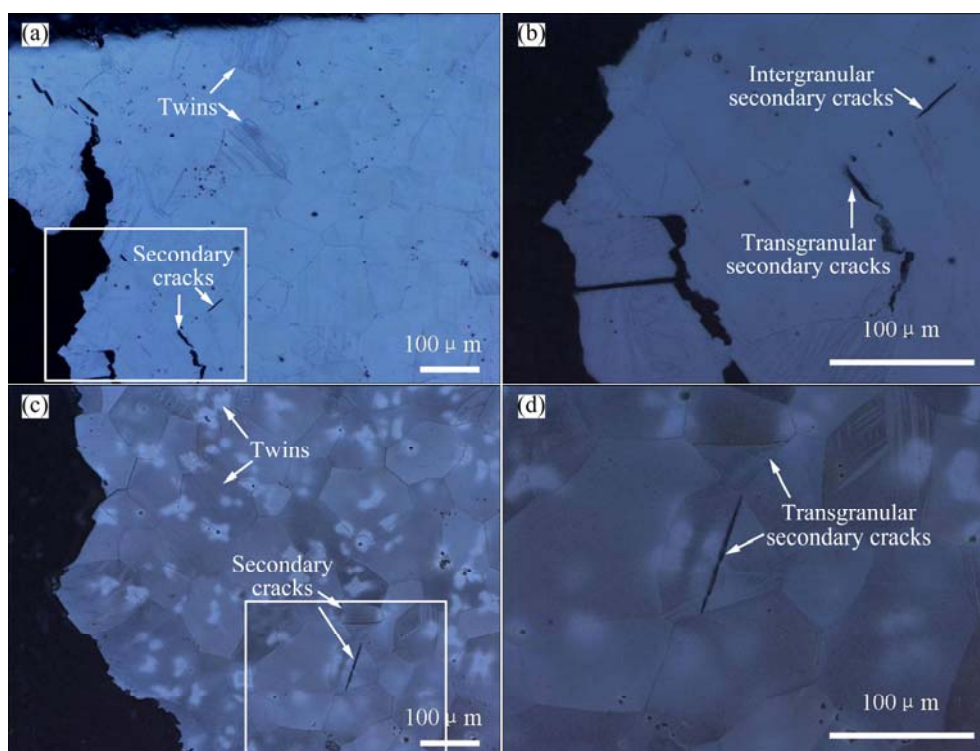


Fig. 11 Optical micrographs showing fracture surface of age-treated GW103K alloy under different aging conditions: (a) Peak-aging at 225 °C; (b) Magnified view of boxed region in (a); (c) Peak-aging at 250 °C; (d) Magnified view of boxed region in (c)

which five independent slip systems necessary for arbitrary shape change are not easily activated at room temperature [21]. The secondary crack has a close relation with twinning. The microcracks may initiate and spread along the twins to form the transgranular cracks.

4 Conclusions

1) The microstructure of the sand-cast Mg–10Gd–3Y–0.5Zr alloy mainly consists of α -Mg and eutectic compound $Mg_{24}(Gd,Y)_5$. After solution treatment, the main composition is α -Mg and γ phase. β' phase gradually precipitates with the progress of aging.

2) Considerable precipitation hardening is exhibited by aging treatment. The Mg–10Gd–3Y–0.5Zr alloy solution treated at 525 °C for 12 h reaches the peak hardness of HV120.9 and HV110.9 aged at 225 °C for 14 h and 250 °C for 12 h respectively. The yield strength, ultimate tensile strength and elongation reach 251.6 MPa, 339.9 MPa, 1.5% and 247.3 MPa, 359.6 MPa, 2.7% at aging conditions of (225 °C, 14 h) and (250 °C, 12 h), respectively. With regards to hardness and tensile properties, the processes of (525 °C, 12 h + 225 °C, 14 h) and (525 °C, 12 h + 250 °C, 12 h) are selected as the optimized heat treatment conditions, respectively.

3) Based on air cooling after heat treatment, the Mg–10Gd–3Y–0.5Zr alloy shows superior function of elongation than the alloy is water cooled after heat

treatment.

4) The fracture modes for the under-aged and peak-aged Mg–10Gd–3Y–0.5Zr alloys are typical transgranular cleavage fracture and transgranular quasi-cleavage fracture, respectively.

References

- [1] LIU Wen-cai, DONG Jie, SONG Xu, BELNOUE J P, HOFMANN F, DING Wen-jiang, KORSUNSKY A M. Effect of microstructures and texture development on tensile properties of Mg–10Gd–3Y alloy [J]. *Materials Science and Engineering A*, 2011, 528(6): 2250–2258.
- [2] POLMEAR I J. Magnesium alloys and applications [J]. *Mater Sci Technology*, 1994, 10(1): 1–16.
- [3] GAO Xiang, HE Shang-ming, ZENG Xiao-qin, PENG Li-ming, DING Wen-jiang, NIE Jian-feng. Microstructure evolution in a Mg–15Gd–0.5Zr (wt.%) alloy during isothermal aging at 250 °C [J]. *Material Science and Engineering A*, 2006, 431(1–2): 322–327.
- [4] NIE Jian-feng, GAO Xiang, ZHU Su-ming. Enhanced age hardening response and creep resistance of Mg–Gd alloys containing Zn [J]. *Scripta Materialia*, 2005, 53(9): 1049–1053.
- [5] GAO Xiang, NIE Jian-feng. Enhanced precipitation–hardening in Mg–Gd alloys containing Ag and Zn [J]. *Scripta Materialia*, 2008, 58(8): 619–622.
- [6] ZHENG Kai-yun, DONG Jie, ZENG Xiao-qin, DING Wen-jiang. Precipitation and its effect on the mechanical properties of a cast Mg–Gd–Nd–Zr alloy [J]. *Material Science and Engineering A*, 2008, 489(1–2): 44–54.
- [7] LIANG Shu-quan, GUAN Di-kai, CHEN Liang, GAO Zhao-he, TANG Hui-xiang, TONG Xu-ting, XIAO Rui. Precipitation and its

- effect on age-hardening behavior of sand-cast Mg–Gd–Y alloy [J]. *Materials and Design*, 2011, 32(1): 361–364.
- [8] LIU Wen-cai, DONG Jie, ZHANG Ping, KORSUNSKY A M, SONG Xu, DING Wen-jiang. Improvement of fatigue properties by shot peening for Mg–10Gd–3Y alloy under different conditions [J]. *Materials Science and Engineering A*, 2011, 528(18): 5935–5944.
- [9] DONG Jie, LIU Wen-cai, SONG Xu, ZHANG Ping, DING Wen-jiang, KORSUNSKY A M. Influence of heat treatment on fatigue behavior of high-strength Mg–10Gd–3Y alloy [J]. *Materials Science and Engineering A*, 2010, 527(21–22): 6053–6063.
- [10] LIU Wen-cai, WU Guo-hua, ZHAI Chun-quan, DING Wen-jiang, KORSUNSKY A M. Grain refinement and fatigue strengthening mechanisms in as-extruded Mg–6Zn–0.5Zr and Mg–10Gd–3Y–0.5Zr magnesium alloys by shot peening [J]. *International Journal of Plasticity*, 2013, 49: 16–35.
- [11] ANYANWU I A, KAMADO S, KOJIMA Y. Creep properties of Mg–Gd–Y–Zr alloys [J]. *Material Transactions*, 2001, 42(7): 1212–1218.
- [12] WANG Qi-long. Study on the microstructure and mechanical properties of sand mould cast Mg–10Gd–3Y–Zr alloy [D]. Shanghai: Shanghai Jiao Tong University, 2010. (in Chinese)
- [13] HE Shang-ming, ZENG Xiao-qin, PENG Li-ming, GAO Xiao-qin, NIE Jian-feng, DING Wen-jiang. Precipitation in a Mg–10Gd–3Y–0.4Zr (wt. %) alloy during isothermal aging at 250 °C [J]. *Journal of Alloys and Compounds*, 2006, 421(1–2): 309–313.
- [14] HE Shang-ming. Study on the microstructural evolution, properties and fracture behavior of Mg–Gd–Y–Zr(–Ca) alloys [D]. Shanghai: Shanghai Jiao Tong University, 2007. (in Chinese)
- [15] DRITS M E, ROKHLIN L L, NIKITINA N I. State diagram of the Mg–Y–Gd system in the range rich in magnesium [J]. *Izvestiia Akademii Nauk SSSR Metally*, 1983, 5: 215–219.
- [16] GAO Lei, CHEN Rong-shi, HAN En-hou. Microstructures and strengthening mechanisms of a cast Mg–1.48Gd–1.13Y–0.16Zr (at. %) alloy [J]. *Journal of Material Science*, 2009, 44(16): 4443–4454.
- [17] HONMA T, OHKUBO T, HONO K, KAMADO S. Chemistry of nanoscale precipitates in Mg–2.1Gd–0.6Y–0.2Zr (at.%) alloy investigated by the atom probe technique [J]. *Materials Science and Engineering A*, 2005, 395(1–2): 301–306.
- [18] GAO Lei, CHEN Rong-shi, HAN En-hou. Fracture behavior of high strength Mg–Gd–Y–Zr magnesium alloy [J]. *Transactions of Nonferrous Metals Society of China*, 2010, 20(7): 1217–1221.
- [19] PENG Qiu-ming, HOU Xiu-li, WANG Li-dong, WU Yao-ming, CAO Zhan-yi, WANG Li-min. Microstructure and mechanical properties of high performance Mg–Gd based alloys [J]. *Materials and Design*, 2009, 30(2): 292–296.
- [20] GAO Lei, CHEN Rong-shi, HAN En-hou. Effects of rare-earth elements Gd and Y on the solid solution strengthening of Mg alloys [J]. *Journal of Alloys and Compounds*, 2009, 481(1–2): 379–384.
- [21] LIU Zhi-jie, WU Guo-hua, LIU Wen-cai, PANG Song, DING Wen-jiang. Effect of heat treatment on microstructures and mechanical properties of sand-casting Mg–4Y–2Nd–1Gd–0.4Zr magnesium alloy [J]. *Transactions of Nonferrous Metals Society of China*, 2012, 22(7): 1540–1548.

热处理对砂型铸造 Mg–10Gd–3Y–0.5Zr 镁合金 微观组织和力学性能的影响

曹 樑¹, 刘文才^{1,2}, 李中权³, 吴国华^{1,2}, 肖 旅³, 王少华⁴, 丁文江^{1,2}

1. 上海交通大学 轻合金精密成型国家工程研究中心, 上海 200240;

2. 上海交通大学 金属基复合材料国家重点实验室, 上海 200240;

3. 上海航天精密机械研究所, 上海 201600;

4. 空间物理重点实验室, 北京 100076

摘 要: 采用金相分析、SEM、硬度试验和拉伸试验等方法分析和测试砂型铸造 Mg–10Gd–3Y–0.5Zr 镁合金在 T6 态(固溶后空冷然后时效)下的显微组织和室温力学性能, 讨论该合金的断裂机理。结果表明, 砂铸 Mg–10Gd–3Y–0.5Zr 合金在 225 °C 和 250 °C 时效下的最优 T6 热处理工艺分别为(525 °C, 12 h+225 °C, 14 h)和(525 °C, 12 h+250 °C, 12 h)。峰时效下 T6 态 Mg–10Gd–3Y–0.5Zr 合金主要由 α -Mg+ γ + β' 相组成, 2 种峰时效热处理工艺下合金的抗拉强度、屈服强度和伸长率分别为 339.9 MPa、251.6 MPa、1.5%及 359.6 MPa、247.3 MPa、2.7%。在不同热处理工艺下 Mg–10Gd–3Y–0.5Zr 合金断裂的类型不同, 峰时效态合金的断裂方式为穿晶准解理断裂。

关键词: Mg–10Gd–3Y–0.5Zr; 镁合金; 热处理; 断裂; 微观组织; 力学性能

(Edited by Xiang-qun LI)